

An Improved Tokamak Sawtooth Benchmark for 3D Nonlinear MHD

J. A. Breslau^{1,*}, C. R. Sovinec² and S. C. Jardin¹

¹ Princeton Plasma Physics Laboratory, P. O. Box 451, Princeton, NJ 08543, USA.

² College of Engineering, University of Wisconsin-Madison, 1500 Engineering Drive, Madison, WI 53706-1609, USA.

Received 31 October 2007; Accepted (in revised version) 17 March 2008

Available online 21 April 2008

Abstract. Accurate prediction of the sawtooth cycle [1] is an important test for nonlinear MHD codes. The sawtooth cycle in the CDX-U tokamak [2], chosen because its small size and low temperature allow simulation using actual device parameters, has been an important benchmark for the comparison of the M3D [3] and NIMROD [5] codes for the last several years. Successive comparisons have led to improvements and refinements in both codes. The most recent comparisons show impressive agreement between the two codes both on the linear instability and on the details of nonlinear cyclical behavior. These tests are somewhat idealized and do not yet agree quantitatively with the experimentally observed sawtooth period. We expect a second generation of CDX-U sawtooth benchmarks based on an analytically specified equilibrium, with source terms that show greater fidelity to the physical device, to produce better agreement.

PACS: 52.55.Fa, 52.65.Kj

Key words: Macroscopic MHD stability, nonlinear MHD, MHD code verification.

1 Introduction

Verification and validation of 3D nonlinear MHD initial value codes is a particularly challenging task. The inherent high sensitivity of nonlinear systems to small differences in initial conditions makes it difficult to distinguish the effects of differences in representation or time-advance scheme from differences in fidelity to the physical model when making detailed comparisons of the predictions of two different codes for a particular instability or other event. It is still more difficult to compare such predictions directly

*Corresponding author. *Email addresses:* jbreslau@pppl.gov (J. A. Breslau), csvinec@cae.wisc.edu (C. R. Sovinec), sjardin@pppl.gov (S. C. Jardin)

with experimental observations, for which measurement error leads to far greater uncertainty regarding the initial conditions. Nevertheless, such efforts are necessary to justify confidence in the predictive capabilities of these codes.

A program of verification and validation has been undertaken for the two workhorse 3D MHD codes of the SciDAC Center for Extended MHD Modeling (CEMM) [4], M3D [3] and NIMROD [5]. The nonlinear instability chosen for the test is the resistive internal kink mode that gives rise to the sawtooth crash [1], a fundamental dynamic of the inductive tokamak discharges these codes are intended to model. The crash involves magnetic reconnection across a thin helical current sheet, a structure whose size varies roughly inversely with the plasma temperature. For large magnetic fusion experiments, the high temperatures result in a current sheet too thin to be practically resolved by present-day codes. Some small tokamaks, however, such as CDX-U [2], are cold enough to have resolvable current layers and hence make good targets for validation studies using actual device parameters. CDX-U was thus chosen for this study.

In this article, we present results of the first successful CEMM cross-code nonlinear verification benchmark: the CDX-U sawtooth cycle. Because this problem should also be of value to the larger MHD modeling community, we also propose a new version of the benchmark with an analytically specified initial state. Preliminary results with this new equilibrium are then presented.

2 Statement of the problem

The CDX-U tokamak is a small ($R_0 = 33.5$ cm), low-aspect-ratio ($R_0/a = 1.5$) device with a typical operating temperature of about $T_e = 100$ eV. Modeling 3D macroscopic activity in the experiment requires the specification of an initial equilibrium as well as sources and transport coefficients. The initial equilibrium configuration and sources are provided by running the 2D transport timescale code TSC [6] to match typical traces of the plasma current $I_p(t)$ from the experiment. A sequence of experimentally relevant equilibria, each at a fixed time, are obtained from the TSC computation as described in [7]. We note that as the central current density increases in the TSC calculation, the central safety factor q_0 , a measure of the pitch of the local magnetic field, falls below unity, the condition for onset of the resistive internal kink instability. A single kink-unstable TSC equilibrium is then chosen to be used as the initial condition for a complete run of each of the two 3D nonlinear codes. For the initial benchmark, we initialized the 3D codes with an equilibrium in which $q_0 = 0.92$.

Both M3D and NIMROD are parallel 3D nonlinear magnetohydrodynamic (MHD) codes in toroidal geometry, solving a superset of the resistive MHD equations that describe the behavior of a collisional magnetized plasma on timescales long compared to electrostatic oscillations but typically short compared to resistive diffusion. The equa-

tions solved by each code are (mks units)

$$\frac{\partial \rho}{\partial t} + \nabla \cdot (\rho \mathbf{v}) = 0, \quad (2.1)$$

$$\rho \left(\frac{\partial \mathbf{v}}{\partial t} + \mathbf{v} \cdot \nabla \mathbf{v} \right) = \mathbf{J} \times \mathbf{B} - \nabla p + \mu \nabla^2 \mathbf{v}, \quad (2.2)$$

$$\frac{\partial \mathbf{B}}{\partial t} = \nabla \times (\mathbf{v} \times \mathbf{B} - \eta \mathbf{J}), \quad (2.3)$$

$$\mu_0 \mathbf{J} = \nabla \times \mathbf{B}, \quad (2.4)$$

$$\frac{\partial p}{\partial t} + \mathbf{v} \cdot \nabla p = -\gamma p \nabla \cdot \mathbf{v} + \nabla \cdot \left[\kappa_{\parallel} \nabla_{\parallel} \left(\frac{p}{\rho} \right) + \kappa_{\perp} \nabla_{\perp} \left(\frac{p}{\rho} \right) \right]. \quad (2.5)$$

Here ρ is the number density, \mathbf{v} is the bulk velocity, \mathbf{J} is the current density, \mathbf{B} is the magnetic field, p is the pressure, μ is the viscosity, η is the resistivity, $\gamma = 5/3$ is the ratio of specific heats, and κ_{\parallel} and κ_{\perp} are coefficients of heat diffusion perpendicular and parallel to the magnetic field respectively.

While they solve the same equations, the two codes differ in the variables being advanced in time, in the method of discretization, and in the numerical algorithms employed. In the M3D code, the magnetic field is kept divergence-free analytically by the use of potential functions: substituting

$$\mathbf{B} = \nabla \psi \times \nabla \phi + \frac{1}{R} \nabla_{\perp} F + (R_0 + \tilde{I}) \nabla \phi, \quad (2.6)$$

into (2.3), where ϕ is the toroidal angle, results in equations for advancing the poloidal flux ψ and the non-vacuum toroidal field \tilde{I} in time along with the auxiliary elliptic solve

$$\nabla_{\perp}^2 F = -\frac{1}{R} \frac{\partial \tilde{I}}{\partial \phi}. \quad (2.7)$$

In NIMROD, the field is represented using the primitive variables, and a diffusion-based method is used to minimize magnetic divergence errors [5]. Both codes use finite element approaches on 2D poloidal meshes, but M3D uses linear basis functions on an unstructured triangular mesh whereas NIMROD uses high-order finite elements on a structured rectangular mesh. In NIMROD, the toroidal dimension has a spectral representation, with each 2D mesh corresponding to a particular toroidal mode number, while M3D uses finite differences toroidally, with each 2D mesh corresponding to a particular value of toroidal angle ϕ . In NIMROD, the linear terms of (2.1)-(2.5) that apply to individual mode numbers and the nonlinear terms that couple different modes together are computed separately, while in M3D these terms are not separated. The NIMROD time advance for the linear terms is fully implicit while M3D's scheme is only partially implicit, with a time step limited by the Courant condition on the shear Alfvén wave. As a result of these design choices, NIMROD is considerably more efficient than M3D at

computing linear modes but potentially less so in the nonlinear regime when several different toroidal harmonics reach comparable amplitudes. NIMROD typically runs faster on cases like the one described here.

For the initial benchmark, a non-evolving Spitzer resistivity profile of the form

$$\eta \propto T_{eq}^{-3/2}$$

was used, normalized so that the central Lundquist number

$$S \equiv \frac{\tau_R}{\tau_A} = \frac{a^2 B_T}{\eta R_0} \sqrt{\frac{\mu_0}{\rho}} = 1.94 \times 10^4.$$

The viscosity was held constant and uniform with a central Prandtl number $\mathbf{P}_N \equiv \mu/\eta$ of 10. A high, uniform, and constant value of κ_\perp was chosen, equivalent to a physical value of approximately 200 m²/s. The two codes differ in their implementation of parallel heat diffusion, with M3D using an ‘‘artificial sound wave’’ method in which a hyperbolic rather than parabolic operator convects heat along the field while NIMROD evaluates the actual diffusion term in (2.5). The parallel heat conduction parameter could therefore only be approximately similar in the two runs; it was chosen to correspond to an electron thermal speed six times the Alfvén speed. As a substitute for Ohmic heating and inductive current drive, source terms were added in the field (2.3) and energy (2.5) equations to drive these respective profiles toward their initial values, i.e., in the M3D code

$$\dot{\psi} = \dots + \eta \Delta^* \psi \quad (2.8)$$

becomes

$$\dot{\psi} = \dots + \eta \Delta^* (\psi - \psi_0), \quad (2.9)$$

where ψ_0 is the initial poloidal flux, presumed to be the equilibrium value, and similarly for the toroidal field and temperature variables. These sources remain switched on at constant strength throughout the duration of the simulation.

3 Initial study

The first comparison made was of the linear $n=1$ eigenmode structure and growth rates. Agreement here was good (Fig. 1). Both codes found the most unstable $n=1$ mode to have dominant poloidal mode number $m=1$ (the expected internal kink mode localized interior to the $q=1$ surface). M3D predicted a normalized growth rate of $\gamma\tau_A=5.1 \times 10^{-3}$, and NIMROD $\gamma\tau_A=4.4 \times 10^{-3}$. Both codes found the equilibrium to be stable with respect to all higher- n modes at the chosen κ_\perp .

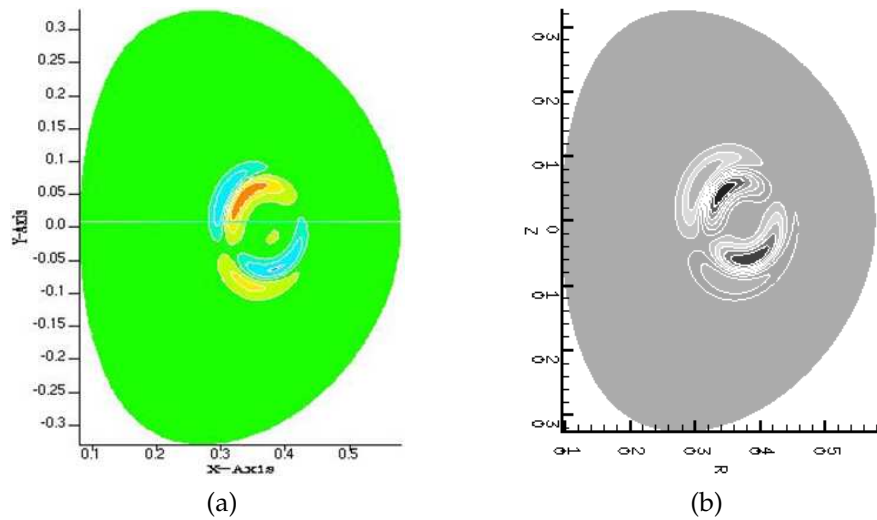


Figure 1: Filled contour plots of toroidal current density on a constant- ϕ section for the $n=1$ eigenmode of the $q_0=0.92$ CDX-U equilibrium. (a) M3D result. (b) NIMROD result.

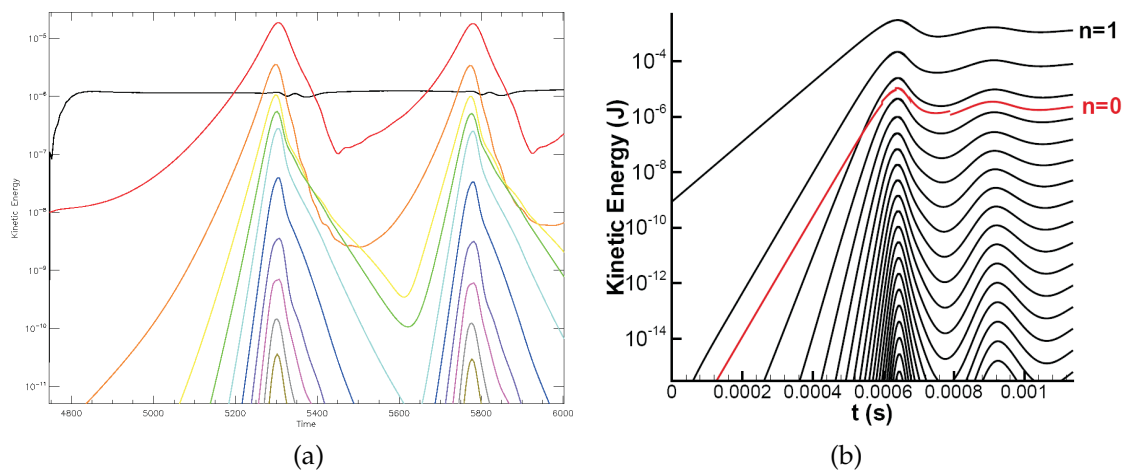


Figure 2: Time history of kinetic energy by toroidal mode number during the first two sawtooth crashes in an earlier iteration of the nonlinear CDX-U benchmark. (a) M3D result (normalized units). (b) NIMROD result (mks units). Highest peaks in both plots are for $n=1$; successively lower peaks are in order of increasing n , except for $n=0$, which is the curve at constant K.E. = 1.2×10^{-6} in a and is labeled in b.

The initial nonlinear comparison was less successful. A previously published set of results from M3D reproduces many of the expected features of the sawtooth cycle [7] but shows disagreement with the NIMROD prediction (Fig. 2).

While the observation of Kadomtsev reconnection [8], temperature flattening, and repeating cycles was promising, this attempt had to be regarded as a failure with respect to code verification. As illustrated in the figures, the two predictions did not agree on the

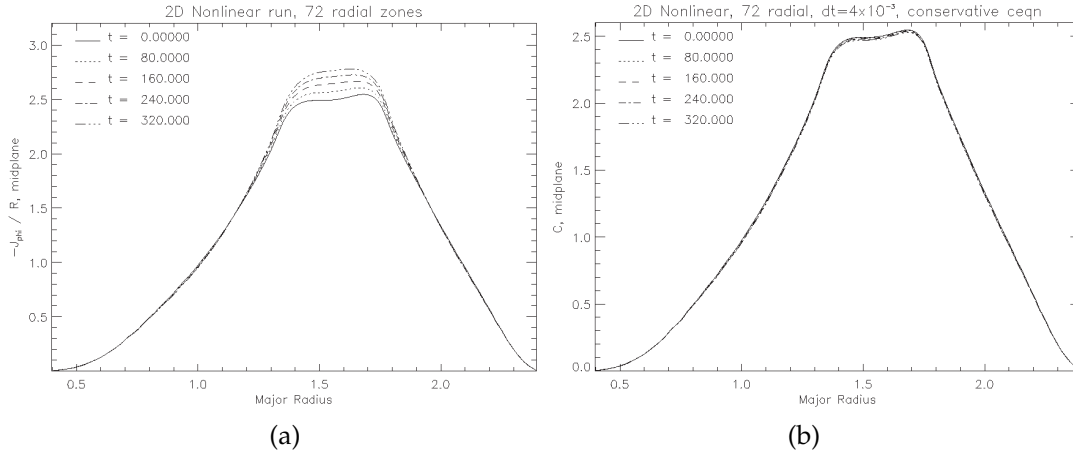


Figure 3: Profile of toroidal current density along midplane at several times during nonlinear 2D M3D run beginning with unperturbed CDX-U equilibrium. (a) Original C equation. (b) Improved, conservative C equation.

degree of damping of oscillation strength between crashes, on the sawtooth period: 480 Alfvén times ($160 \mu\text{s}$) for M3D vs. $800 \tau_A \approx 266 \mu\text{s}$ for NIMROD. Nor was there close agreement on the growth rate of the $n=1$ mode in the linear phase, which remains constant in NIMROD but increases in time significantly in M3D. Further, there were indications that the M3D case was under-resolved and not convergent as the number of toroidal zones was increased.

The changing growth rate effect in M3D was found to arise from an unphysical steady decrease in the central value of the safety factor q_0 arising from poor conservation properties of M3D's treatment of toroidal current density in the presence of a current source term and equilibrium flow. This poor conservation was shown to result in a significant increase in the central current density over time (and hence a decrease in q_0) even in a two-dimensional nonlinear simulation with no $n=1$ activity. It arose numerically from a scheme in which the elliptic operator

$$\Delta^* \equiv R^2 \nabla \cdot \left(\frac{1}{R^2} \nabla \right)$$

applied to the expression for the rate of change of the poloidal flux function $\psi(\mathbf{x}, t)$ was evaluated algebraically and then assembled term by term to compute the rate of change of the toroidal current density function

$$C \equiv -R J_\phi = \Delta^* \psi + \frac{1}{R} \frac{\partial F}{\partial z}.$$

Following the first M3D-NIMROD comparison, it was realized that much more accurate conservation could be achieved by composing ψ term by term instead and then evaluating the elliptic operator on the sum of the terms numerically. Fig. 3 illustrates the improvement in conservation accomplished by this change.

Other improvements that were found to be required included the substitution of an isotropic viscosity operator in M3D for the perpendicular operator that was originally in use; and a more accurate equilibrium calculation in NIMROD in which the parallel component of the current density was recomputed from the equilibrium magnetic field on initialization rather than interpolated from the input file using cubic splines. Finally, a scaling study in q_0 revealed that the $n = 1$ growth rate was highly sensitive to this parameter and that the $q_0 = 0.92$ equilibrium was very close to marginal stability with the transport coefficients listed earlier, making detailed agreement especially challenging. Accordingly, a different initial equilibrium was extracted from the same TSC sequence, with $q_0 = 0.82$, making it further from marginal stability and thus more robustly unstable. It was found that the codes were now in satisfactory agreement on the $n = 1$ eigenmode and growth rate.

4 Agreement

The results obtained after the aforementioned fixes are shown for comparison in Fig. 4. It is clear from the figure that the codes are now in substantial, detailed agreement. Like NIMROD, M3D now conserves q_0 in the absence of mode activity, and thus shows a constant linear growth rate for the $n = 1$ mode until just before the first crash. The codes also agree in the relative magnitudes of the various toroidal modes before, during, and after the crashes; on the detailed time behavior of the low- n modes; on the degree of damping of the oscillation in successive cycles, and on the cycle period of $\sim 600\tau_A$ ($200 \mu\text{s}$). It has also been confirmed that the M3D result is now converged toroidally.

When we investigate the actual plasma state at various corresponding times in the two runs, we also find detailed agreement (Figs. 5-6). This agreement constitutes a successful verification of the two codes. However the present modeling is insufficient to produce quantitative agreement with the experimental results for the two predictions that can be compared directly with soft X-ray data from the experiment: the sawtooth period and the crash time. The predicted period of $200 \mu\text{s}$ is significantly less than the observed $500 \mu\text{s}$ sawtooth period in CDX-U, and the predicted crash time is a much larger fraction of the total cycle time than is observed in the device. Hence this study cannot be considered a successful validation of the model. It appears likely that an explanation for the discrepancy in time scales must come at least in part from the artificial nature of the source terms used, e.g., in (2.9). A more refined model and a set of initial and boundary conditions that show greater fidelity to the experimental conditions are therefore required.

5 Conclusions and future plans

Our original study demonstrated that detailed nonlinear 3D MHD simulation of the sawtooth cycle with representative device parameters was possible for a small device and

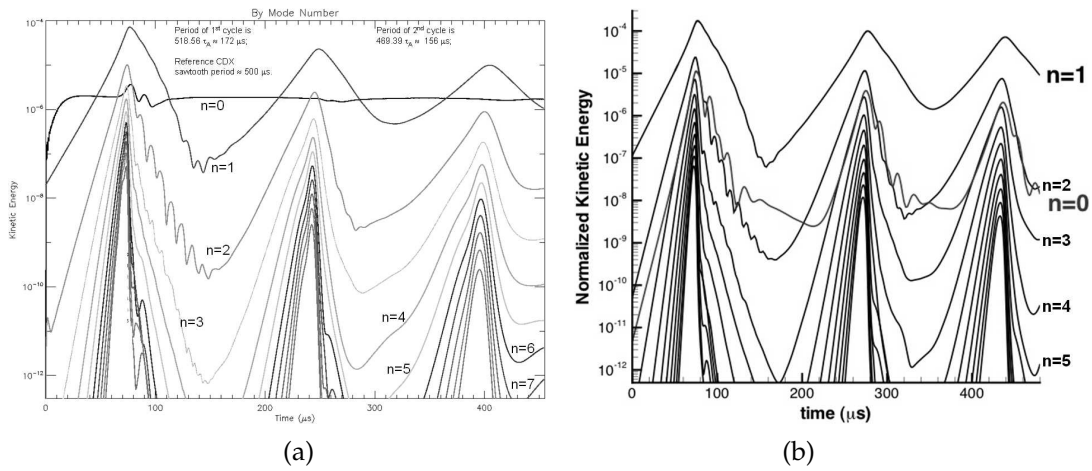


Figure 4: Time history of normalized kinetic energy by toroidal mode number during the first three sawtooth crashes in the present iteration of the nonlinear CDX-U benchmark. (a) M3D result. (b) NIMROD result.

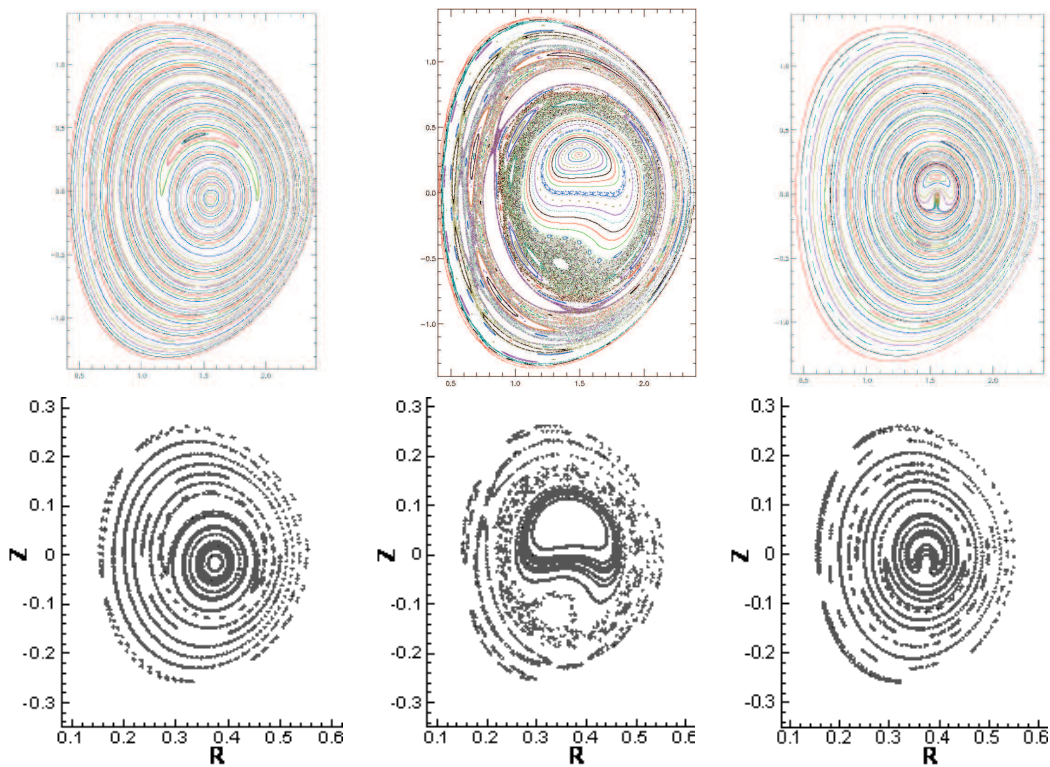


Figure 5: Poincaré sections showing magnetic flux surfaces at several time instants during the M3D (top) and NIMROD (bottom) sawtooth cycles. Left: late linear phase. Center: at culmination of crash. Right: Early recovery phase following crash.

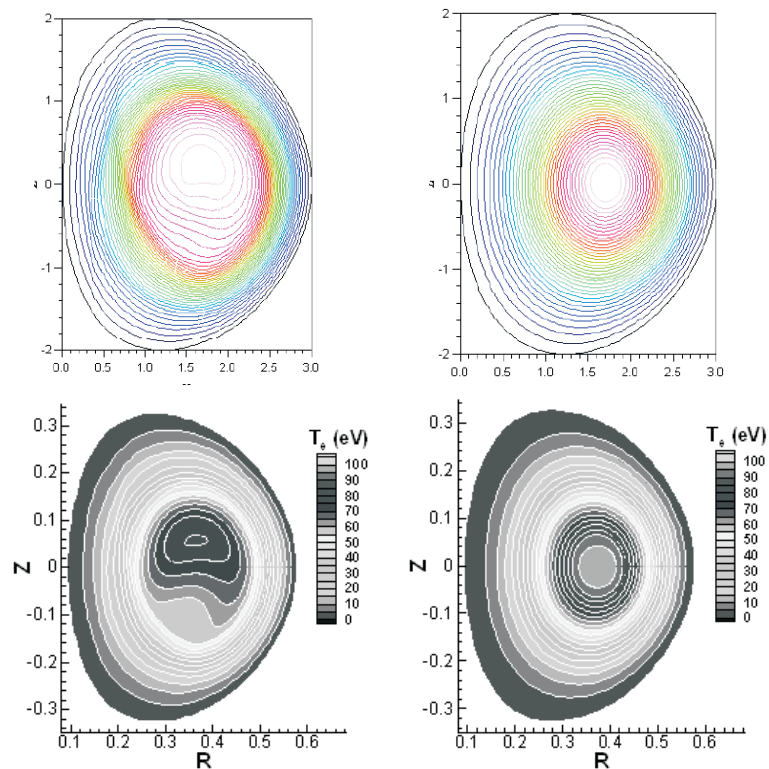


Figure 6: Temperature contours at two times during the M3D (top) and NIMROD (bottom) sawtooth cycles. Left: at culmination of crash. Right: Early recovery phase following crash.

with sufficient computing power, and that it was capable of reproducing qualitatively all the salient features of the instability. We have now shown that cross-code verification is possible in the nonlinear regime as well, with close quantitative agreement achieved in spite of the numerous differences in numerical implementation. This exercise was extremely valuable for both groups of developers in that it led to greater understanding (and in many cases improvements) of each code's behavior, and ultimately to enhanced confidence in the accuracy of their predictions. It also illustrated the necessity of thorough, clear communication in the preparation of such a complex nonlinear benchmark.

Based on the lessons learned in the successful verification exercise, and out of a desire for a successful validation as well, we propose a new more rigorous and more physically valid test based on the same instability. The next iteration of the CDX-U sawtooth benchmark matches the physics of the experiment more closely in terms of boundary conditions, sources, and transport coefficients so that these differences do not interfere with a successful validation. The new initial equilibrium state is defined in a simple analytic way, enabling any other nonlinear predictive tokamak MHD code to be tested on the same problem, making possible a standard community-wide benchmark.

CDX-U is a small, inductively-driven short-pulse tokamak without any auxiliary heat-

Table 1: Parameters for the next equilibrium for the CDX-U sawtooth benchmark.

Quantity	Value
Major radius R_0	0.341 m
Minor radius a	0.247 m (aspect ratio = 1.38)
Ellipticity κ	1.35
Triangularity δ	0.25
Central temperature ($T_e = T_i$)	100 eV
Normalized central pressure $\mu_0 p_0$	7.5×10^{-4} (implies $n_{e0} = n_{i0} = 1.863 \times 10^{19} \text{ m}^{-3}$)
α Parameter in pressure equation*	0.1
Vacuum value g_0 of $R \cdot B_T$	0.04252 T · m
Effective ion charge Z_{EFF}	2.0
Loop voltage V_L	3.1741 V (implies $q_0 \approx 0.82$)

* $p(\psi) = p_0[\alpha\tilde{\psi} + (1-\alpha)\tilde{\psi}^2]$, where $\tilde{\psi} \equiv (\psi - \psi_{\text{limiter}}) / (\psi_{\text{axis}} - \psi_{\text{limiter}})$.

ing or current drive sources. In contrast, the heat and current sources present in the previous test always drive these profiles toward their initial equilibrium states, which is unphysical. For this iteration, all heating is now self-consistent ohmic heating, with a resistivity profile that evolves to track the temperature with a $T^{-3/2}$ dependence, rather than remaining static as before. The very high, uniform perpendicular heat conduction is replaced by a static profile that more accurately represents what was inferred from the experiment. Current drive is now purely inductive, with a loop voltage applied as a boundary condition and regulated to provide constant power input during the run.

The new equilibrium is specified analytically in Table 1 and may be computed with any equilibrium code, such as JSOLVER [9]. The initial, uniform loop voltage is that needed to drive the initial toroidal current against the initial resistance:

$$V_{loop} = \frac{2\pi\eta \langle \mathbf{J} \cdot \mathbf{B} \rangle}{\langle \mathbf{B} \cdot \nabla \phi \rangle}, \quad (5.1)$$

where the brackets denote the flux surface average. Subsequently, the voltage should track the evolving current to maintain constant input power. The perpendicular heat conduction profile should be computed self-consistently to provide a steady state in the presence of the ohmic heating arising from the current density and temperature distributions — if the random heat flux is

$$\mathbf{q} = -\kappa_{\perp} \nabla_{\perp} T,$$

then we can integrate the surface average of the energy equation to get

$$\kappa_{\perp} = \frac{1}{T' \langle |\nabla \psi|^2 \rangle} \left[\frac{V_{loop}}{2\pi\mu_0} \left\langle \frac{|\nabla \psi|^2}{R^2} \right\rangle \right], \quad (5.2)$$

where the prime denotes the derivative with respect to the poloidal flux function ψ and the particle flux corresponding to Pfirsch-Schlüter diffusion has been neglected.

The plasma boundary is parameterized as follows based on the values in the table:

$$\begin{aligned} R(\theta) &= R_0 + a \cos[\theta + \delta \sin(\theta)], \\ z(\theta) &= a \kappa \sin(\theta). \end{aligned} \quad (5.3)$$

The temperature profile is taken to be linear in the normalized flux,

$$T(\psi) = T_0 \tilde{\psi}, \quad (5.4)$$

so that the density becomes

$$n(\psi) = \frac{p}{2k_B T} = \frac{p_0}{2k_B T_0} [\alpha + (1 - \alpha) \tilde{\psi}], \quad (5.5)$$

where $k_B = 1.6022 \times 10^{-19}$ J/eV is Boltzmann's constant and the parameter α is defined in Table 1. The Spitzer resistivity profile has a coefficient of $1.06 \times 10^{-6} Z_{EFF} \Omega\text{-m}$, which assumes the Coulomb logarithm $\ln \Lambda = 20$.

Initial axisymmetric nonlinear M3D results with this new equilibrium show promise, confirming that the steady state can be maintained without conventional sources. Preliminary low- n linear results now suggest that this equilibrium is susceptible to the same (1,1) mode as the previous one, and that its higher- n modes are unstable at the same rational surface, with smaller growth rates. We intend to pursue this instability into the nonlinear regime once again with both codes and hope to achieve a three-way agreement between them and the experiment. We also invite other members of the tokamak modeling community to adopt this test problem as a nonlinear benchmark and to share their results.

The goal of this research is ultimately to develop a predictive capability relevant to burning plasma fusion experiments that are much larger and much hotter than CDX-U. While this verification result is gratifying, simple scalings indicate that many orders of magnitude more computing power would be needed to apply these codes to those experiments in a straightforward way using their real physical parameters. While some of this increase may come from future hardware, much of it must be achieved by advances in numerical methods, such as the use of greater implicitness, adaptive mesh refinement, and more efficient linear solvers.

Acknowledgments

The authors would like to thank D. Schnack, S. Kruger, W. Park, G. Fu, J. Chen, H. Strauss, and L. Sugiyama for valuable discussions regarding and contributions to this study. Calculations were performed at the National Energy Research Scientific Computing Center (NERSC), which is supported by the Office of Science of the U.S. Department of Energy

under Contract No. DE-AC02-05CH11231, and at the National Center for Computational Sciences (NCCS). This work was performed under Grants No. DE-AC02-76CH03073 and DE-FC02-02ER54668 with the U.S. Department of Energy.

References

- [1] R.J. Hastie, *Astrophys. Space Sci.* 256 (1997), 177.
- [2] J. Menard, R. Majeski, R. Kaita, et al., *Phys. Plasmas* 6 (1999), 2002.
- [3] W. Park, et al., *Phys. Plasmas* 6 (1999), 1796.
- [4] Documented online at w3.pppl.gov/cemm.
- [5] C.R. Sovinec, A.H. Glasser, T.A. Gianakon, D.C. Barnes, R.A. Nebel, S.E. Kruger, D.D. Schnack, S.J. Plimpton, A. Tarditi, and M.S. Chi, *J. Comput. Phys.* 195 (2004), 355.
- [6] S. Jardin, N. Pomphrey, and J.L. DeLucia, *J. Comput. Phys.* 66 (1986), 481.
- [7] J.A. Breslau, S.C. Jardin, and W. Park, *Phys. Plasmas* 14 (2007), 056105.
- [8] B.B. Kadomtsev, *Sov. J. Plasma Phys.* 1 (1975), 389.
- [9] J. DeLucia, S.C. Jardin, and A.M.M. Todd, *J. Comput. Phys.* 37 (1980), 183.